

UNCLASSIFIED

Seeker Testing and Facility Improvements in the AEDC 7V Sensor Chamber

W. R. Simpson and R. A. Nicholson
Sverdrup Technology, Inc., AEDC Group
Arnold Engineering Development Center
Arnold Air Force Base, Tennessee 37389

Approved for public release; distribution unlimited.

19970912 096

DTIC QUALITY INSPECTED 2

AIAA/BMDO Technology Conference

August 1997 / San Diego, CA

UNCLASSIFIED

UNCLASSIFIED

SEEKER TESTING AND FACILITY IMPROVEMENTS IN THE AEDC 7V SENSOR CHAMBER*

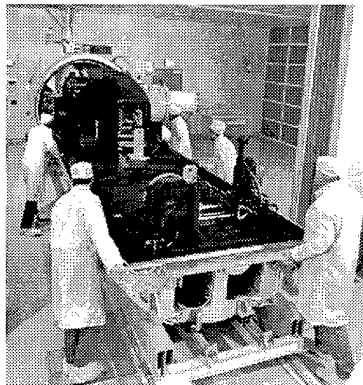
W. R. Simpson** and R. A. Nicholson**
Sverdrup Technology, Inc., AEDC Group
Arnold Engineering Development Center
Arnold Air Force Base, TN 37389-6400

ABSTRACT

An advanced seeker test facility at the Air Force's Arnold Engineering Development Center (AEDC) has been used for the past two years for calibration and performance characterization of infrared seekers supporting Army interceptor programs. This facility, known as the 7V Chamber, is part of a broad range of test capabilities developed at AEDC to provide comprehensive ground test support to the Kinetic Kill Vehicle (KKV) community. The 7V is a state-of-the-art cryo/vacuum facility providing calibration and high-fidelity mission simulation against complex backgrounds. This paper briefly reviews the 7V test capabilities, as well as a number of improvements recently completed or under development.

INTRODUCTION

AEDC, located at Arnold Air Force Base, TN, offers a wide range of advanced aerospace ground test capabilities for the DoD and civilian community. The Space Test Complex provides a number of space simulation facilities, including a low-background infrared sensor test capability in the 7V Chamber. Although the 7V Chamber, shown in Fig. 1, can test both advanced interceptor seekers and surveillance sensors, this paper concentrates on seeker testing. A thorough description of the 7V Facility is given in Ref. 1; therefore, only the following key features are presented to highlight the updates to the facility capability made over the last two years:



- High-fidelity scene system for target clusters, closely spaced objects, and blooming targets allowing independent control of target radiance, spectral content, position, and motion rates,
- Complex scene generation with a high-resolution, heated-pixel array source,
- In-situ scene monitoring with NIST-traceable radiometric and goniometric target calibration,
- Near-visible quality all-reflective optics with a high-speed scan mirror for miss-distance simulation, and
- High-speed, three-axis positioner for pitch/roll/yaw seeker alignment and attitude corrections.

In addition to these capabilities, a number of improvements have been made to the 7V facility or are in development (see Ref. 2) at the present time:

- Added an overlaid visible band with variable intensity to one of the closely spaced object targets,
- Added an Earth Limb Background Source,
- Added another Uniform Flood Source using an isothermal heated black plate,

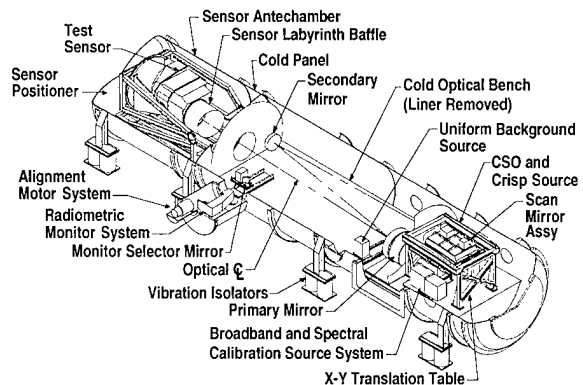


Fig. 1. 7V Sensor Test Facility.

* The research reported herein was performed by the Arnold Engineering Development Center (AEDC), Air Force Materiel Command. Work and analysis for this research were performed by personnel of Sverdrup Technology, Inc., AEDC Group, technical services contractor for AEDC. Further reproduction is authorized to satisfy needs of the U. S. Government.

** Member, AIAA.

This paper is declared a work of the U. S. government and not subject to copyright protection in the United States.

Approved for public release; distribution unlimited.

UNCLASSIFIED

- Improved the heated pixel source with neutral density filters to simulate mission range target intensity,
- Completed a radiometric calibration of the heated pixel scene generator,
- Improved goniometric calibration of target track accuracy,
- Dramatically decreased narcissus problems generated by warm seekers,
- Characterized target systems over a broader spectral range of targets, and
- Improved the optical validation with in-situ measurement of the system point spread function.

FACILITY OVERVIEW

The 7V Chamber is designed to provide advanced calibration and characterization of performance for infrared surveillance and seeker sensors. Characterization includes not only radiometric calibration, but also goniometric calibration to evaluate accuracy of target tracking and guidance commands. The key to evaluation of sensor mission performance is a thorough understanding of its operational characteristics. This includes establishing performance envelopes, defining interrelationships of key variables, identifying non-linear behavior, and measuring timing and sequencing.

The requirements for the 7V were developed by first identifying mission issues and test needs necessary to evaluate seeker performance. The capabilities of the 7V, which satisfy these general seeker test needs, were verified and documented over the last three years with seven cryogenic pumpdowns of the facility since its initial checkout in February 1994. The results of each test have verified the performance parameters and provide an excellent statistical basis for the quoted accuracy and repeatability of the 7V.

Details of the facility infrastructure and data system are given in Ref. 1, this paper concentrates on the simulation capabilities critical to seeker evaluation. As illustrated in Fig. 1, all of the simulation equipment is mounted on a rigid optical bench within the vacuum chamber. For low infrared background, all equipment along with the bench is cryogenically cooled to less than 20 K (higher background tempera-

tures can also be provided, if desired). The test volume is totally enclosed inside a light-tight cryogenic liner. The scene is projected into the sensor under test by reflective collimation optics to simulate the target range. A high-speed scan mirror is also provided in the optical train to sweep the scene across the seeker's field of view and simulate the effects of divert movements in real time. The seeker is mounted on a high-speed, three-axis gimbal support system for initial alignment, calibration of individual detectors, and simulation of attitude movements. The chamber, antechamber, and optical bench provide a rigid structure to control relative line-of-sight (LOS) motions between the scene and the sensor. Jitter is controlled by mounting the entire facility on pneumatic vibration isolators to attenuate seismic inputs and equipment vibrations. Interferometer testing of the optics shows the LOS jitter to be less than 3 μ rad.

SCENE SIMULATION

The primary objective of the 7V scene simulation is high fidelity of target radiometrics and precise location of individual targets or high-density target clusters. The typical mission scene for exo-atmospheric interceptor sensors is illustrated in Fig. 2. Three separate systems are used to provide threat scenarios that can be overlaid on a variable natural space or an earth-limb background:

- Complex cluster(s) of targets expanding from a clump to fully resolved targets,
- Closely Spaced Object (CSO) simulation of two or more targets separating into fully

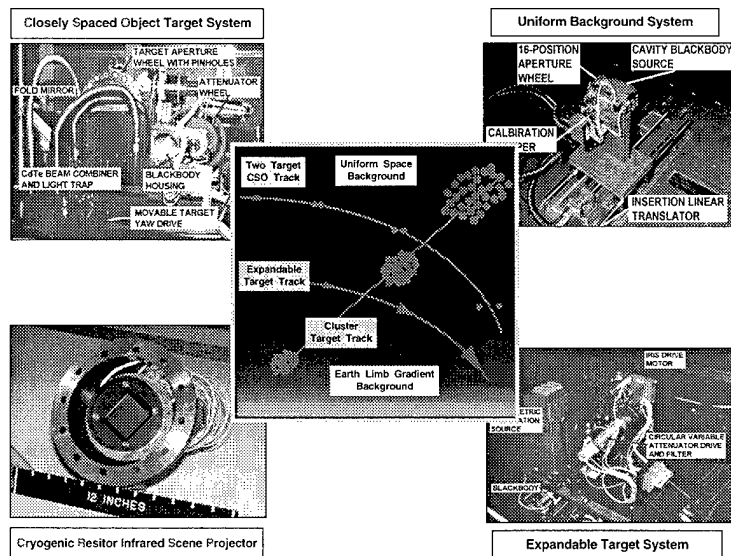


Fig. 2. 7V scene simulation system.

UNCLASSIFIED

resolved targets or a single target separating from a cluster, and

- Blooming triangular or circular targets for end-game simulation

The cluster and CSO target simulations can be tracked across the sensor's field of view on the precision X-Y translator covering a 1.2-deg field of regard at speeds up to 0.5 deg/sec. The endgame target can be moved relative to the seeker line of sight by the high-speed scan mirror at speeds up to 6 deg/sec.

Complex Target Simulation. Simulation of complex target scenarios is provided by a heated pixel scene generator, called CRISP (Cryo/vacuum Resistor Array Infrared Scene Projector). Based on etched silicon micromachining technology, the CRISP generates dynamic patterns of 1 to 400 independent targets using an array of 512 by 512 heated resistor pixels. The microphotograph in Fig. 3 shows several individual 90- μm pixels which subtend 5.3 μrad based on the present collimator. The resistor is supported on top of the addressing and control electronics by a thin silicon bridge which isolates the cold substrate and heat sink to minimize crosstalk. The two-layered structure also increases the fill factor of each pixel to 90 percent. As shown in the schematic of Fig. 3, the combination of a reflector and tuned optical cavity under the pixel and the black titanium nitride emitter surface increases the emittance of each pixel to about 70 percent with spectral characteristics of a graybody. Each heater is individually addressable over an effective temperature range of 20 to almost 500 K with 1 K control. The pixel structure has a thermal time constant of 32 msec. Depending on the requirements of the seeker under test, a point target can be simulated by a subarray of at least 6 by 6 pixels for a 32- μrad target or more for larger targets. By sequentially heating and cooling adjacent pixels, the target appears to move in single pixel steps of 5.3 μrad . Because the composite of 6 by 6 pixels making up a target form a near diffraction-limited image, the target intensity can be varied over a dynamic range of 36 or more at constant temperature. One of the upgrades to the 7V is the addition of a drive system to insert neutral density filters over the CRISP to decrease target intensity and increase its range simulation. The CRISP has been calibrated for uniform response using the Radio-

metric Calibration and Alignment Monitoring Systems, which are described in the Facility Test Results section.

Closely Spaced Object Simulation. The seeker's ability to resolve closely spaced objects into discrete targets is an important test to define mission time lines available to establish track files from target centroids and discriminate decoys and identify targets. As shown in Fig. 4, this capability is provided in the 7V by two integrating sphere graybody sources overlaid with a CdTe beam combiner which has a broadband AR coating to attenuate ghost images. One source moves relative to the other, while both are tracked across the sensor's field of view on the precision X-Y scanner. Each source has independent control of temperature and

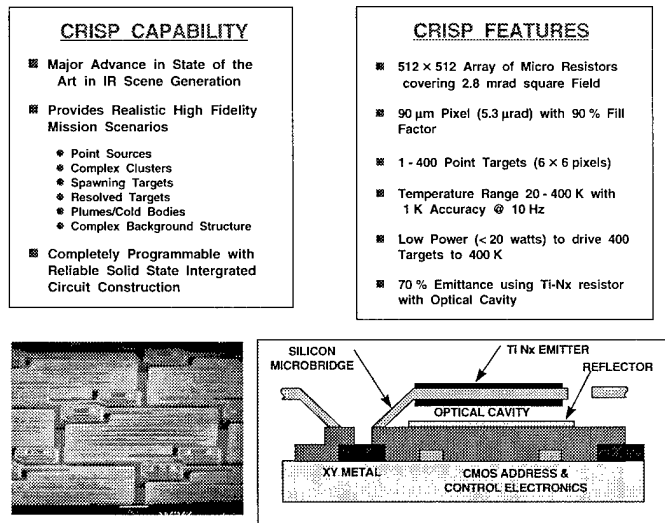


Fig. 3. CRISP Cluster Target System.

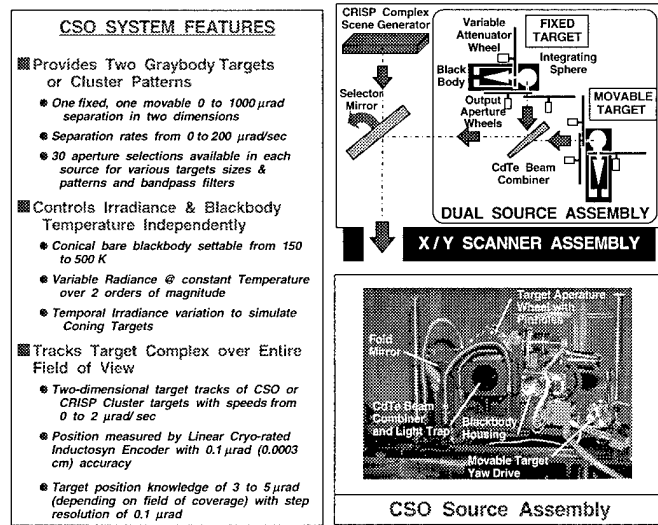


Fig. 4. Closely Spaced Object Target System.

radiometric output, so the effect of target color temperature on seeker performance can be tested at constant intensity. The source intensity of both targets can also be dynamically varied up to four hertz to simulate coning or tumbling targets. For multiple CSO patterns or variable source size, both sources are equipped with output aperture wheels providing up to 30 user-selectable patterns or bandpass filters. Two narrow-band filters are presently installed in one CSO wheel to measure end-to-end point spread function, including all the chamber optical elements using the Alignment Monitor System.

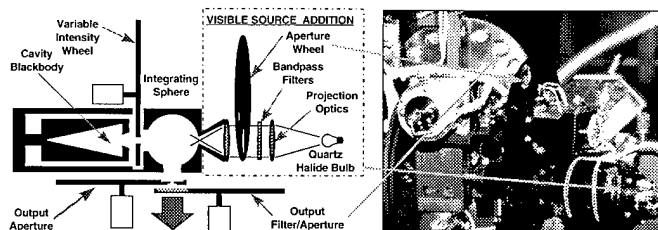
One of the recent upgrades to the CSO source is the addition of a visible band to one target. As shown in Fig. 5, a quartz halide bulb is projected into the integrating sphere of the fixed source by the condenser lens pair. An aperture wheel between the lenses provides nine discrete intensity levels covering over 3 orders of magnitude. The 1.4- μm lenses currently limit the bandpass to 0.5 to 1.4 μm , but cut-on/off filters can be added if narrower bands are necessary.

Expandable Target System. The third scene scenario in Fig. 2 is an expandable target to evaluate seeker endgame target centroiding for aim-point/hit-point determination. As shown in Fig. 6, both circular and triangular targets of various aspect ratios can be simulated by using a dynamic cryogenic iris in conjunction with an aperture wheel. To simulate target intensity increase due to range closing, the source has a ZnSe circular variable attenuator. This wheel provides over two orders of magnitude change of source intensity in real mission time lines. In conjunction with the Scan Mirror, the expandable target can be swept across the seeker field of view at rates up to 6 deg/sec to simulate the effect of miss distance on seeker tracking. This is a valuable feature to test real-time seeker centroiding ability at high closure speeds.

Background Simulation. Variable uniform space backgrounds are provided by directly projecting the output from a blackbody into the seeker entrance aperture. As shown in Fig. 1, the Uniform Background Source (UBS) is located in front of the primary mirror, at the edge of the sensor's field of view. It illuminates the entrance aperture of the sensor, overfilling its focal plane with uniform radiation. The source is a large conical blackbody fitted with an 8-position aperture wheel to vary background intensity

at constant source temperature. The UBS is mounted on a translator stage normally positioned outside the field of view or moved into the edge for a background source. The UBS can also be used on the optical axis for sensor focal plane flood source testing and for establishing non-uniformity correction of the Alignment Monitor camera or a sensor focal plane.

The second background generator currently available in the 7V is an earth limb simulator. It is located out of focus providing an intensity gradient simulating the earth limb. As shown in Fig. 7, this design uses an array of small diameter (0.020 in.) Inconel[®] wires approximately 14 in. long spaced on 0.5-in. centers. Each wire can be heated independently and is fully programmable to cover altitudes up to the 1.4-deg field of view with diurnal or seasonal variation in earth limb intensity. Present scenes are based on SSGM-generated models,



- VISIBLE SOURCE FEATURES**
- Simultaneous overlay with IR source output
 - 2700 K Tungsten filament in a Quartz Halide bulb
 - Variable intensity @ constant source temperature (Intensity @ Sensor = 3×10^{-13} to 2×10^{-16} watts/cm²)
 - Variable bandwidth with low and high pass filters (presently 0.5 to 1.4 μm , peaking @ 0.8 μm)

Fig. 5. Visible band source addition to CSO system.

EXPANDABLE TARGET FEATURES

- Simulates Circular or Triangular Closing Targets
 - Point to 1.5 mrad bloomed size controlled to $\approx 50 \mu\text{m}$
 - Blooming Rate controllable from 0 to 1.5 mrad/sec
- Simulates Closing Target with High Speed Variable Intensity
 - Independent Control of Irradiance at Constant Blackbody Temperature
 - Variable Irradiance with Circular Variable Neutral Density Attenuator with 2 orders of magnitude dynamic range at 0 to 10^{10} W/cm²/sec
 - Conical Bare Blackbody settable from 150 to 500 K
- Simulates Variable Miss Distance of Closing Target with High Speed Target Motion
 - Variable Target Movement from 0 to 6 deg/sec
 - Fully Programmable with Closed Loop Position Control

Expandable Source Mounted to 7V

Fig. 6. Expandable Target System.

but many gradients can be simulated. See Ref. 2 for further details on the analysis and performance of the Earth Limb Background Source.

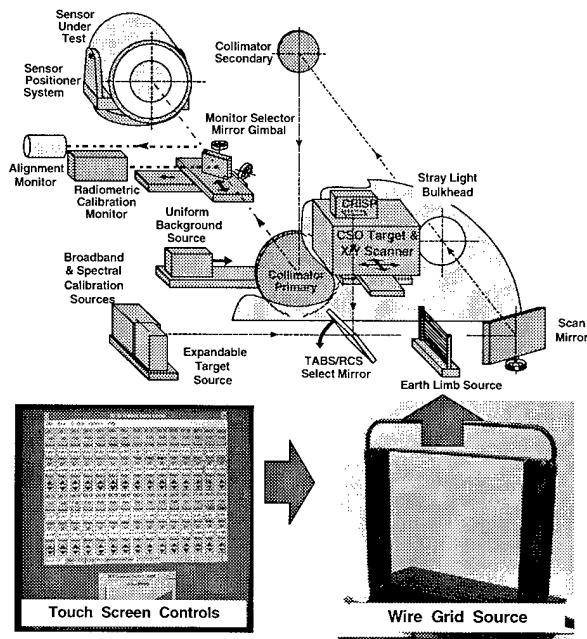


Fig. 7. Earth-limb Background System.

RADIOMETRIC AND GONIOMETRIC CALIBRATION

In-situ calibration of all 7V sources is provided for both radiometric output traceable to the broadband standard of the National Institute of Standards and Technology (NIST) and goniometric target position and track accuracy. As shown in the chamber layout of Fig. 1 and schematically in Fig. 8, the Radiometric Calibration System (RCS) consists of the calibration source for broadband and spectral input to the seeker and the calibration monitor for in-situ measurement of all the source outputs over broadband and spectral regions. The goniometric function is provided by the Alignment Monitor System (AMS), which incorporates an infrared array camera to image the scene projected into the seeker. Both monitors are located in an antechamber just in front of the sensor. Either monitor can be used by deploying a gimbaled flat mirror into the collimated beam to direct radiation into focusing optics which image the scene onto IR detectors for in-situ calibration.

Radiometric Calibration. The RCS Calibration Sources provide several operational modes as point or extended sources with either broadband or spectral output. Low-level, broadband output is

provided from an integrating sphere coupled to a blackbody through a 12-position aperture wheel. This technique provides wide dynamic range of 3 orders of magnitude at any temperature in an operating range of 150 to 500 K. The unisphere source is supplemented by a bare cavity blackbody with variable output aperture for additional output levels at the upper end of the dynamic range. Either source can be attenuated with neutral density filters to lower the dynamic range by an additional one to three orders of magnitude to a minimum irradiance of 10^{-18} W/cm². Including temperature variation, the total dynamic range of the calibration sources is almost eight orders of magnitude. Spectral output is provided by the cavity blackbody filtered by a three-segment Circular Variable Filter (CVF) covering narrow-band energy over 2.5 to 14.5 μ m with bandwidth varying from 1.0 percent at the lower end to 1.8 percent at the upper end.

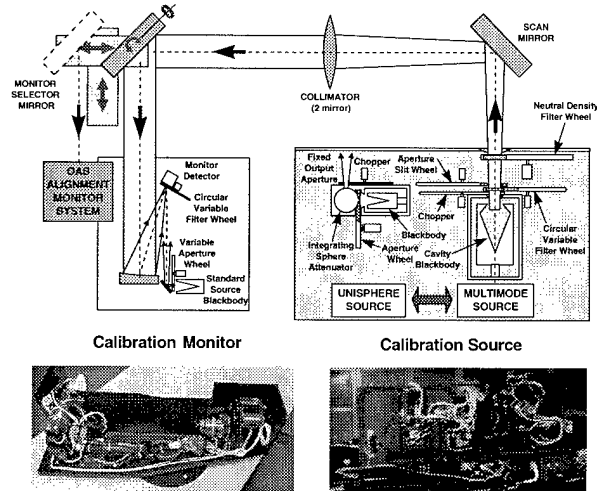


Fig. 8. 7V calibration system layout.

A recent addition to the 7V radiometric calibration capability is an extended source to supplement the UBS for flood source testing of a seeker focal plane. This source, shown in Fig. 9, is a 10-in.-diam aluminum plate, etched and black anodized with an emittance of greater than 0.95 from 3 to 25 μ m. The plate is heated with a single large electrical heater to a uniform temperature in the range from 100 to 350 K. This source is mounted to the monitor selector mirror insertion drive and can be deployed in front of the sensor under test covering its complete field of view. The source temperature is monitored by 6 calibrated platinum temperature sensors mounted around the plate. Preliminary measurements indicate temperature uniformity of less than 1 K.

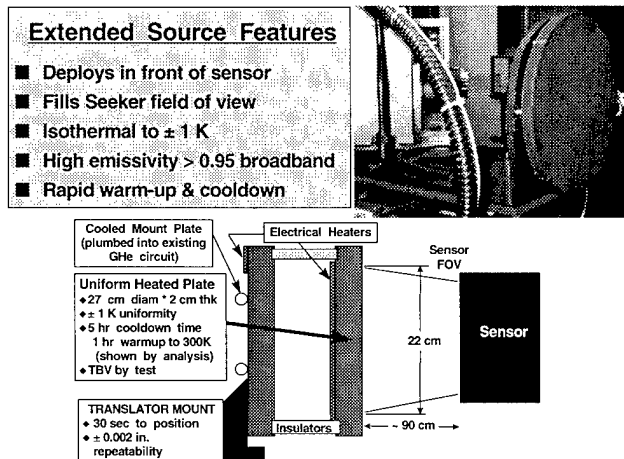


Fig. 9. Flood source heated plate.

The Radiometric Calibration Monitor System, shown on the left side of Fig. 8, samples the output from any source for to measure irradiance in the collimated and its uniformity. To measure radiometric output, the monitor selector mirror reflects part of the collimated radiation into a 10-cm-diam imaging mirror to focus the energy onto a 1-mm-square Gallium-doped silicon detector. The detector, operating at 16 K, responds over a spectral band from 2 to 18 μm . It is calibrated in-situ by a secondary standard blackbody, previously calibrated at NIST to better than 1-percent accuracy. For spectral calibration of any source, a CVF is inserted in front of the Si:Ga detector. An 8- to 14- μm bandpass filter is also installed to aid in improving radiometric calibration accuracy. Typical calibration results are shown in the Facility Test Results section.

Goniometric Calibration. Calibration of target position is accomplished by the Alignment Monitor System (AMS) shown in Fig. 10. This device is a cryogenic infrared camera equipped with a 256×256 Indium Antimonide (InSb) focal plane. In the 7V, the AMS covers a 0.75-deg-square portion of the collimator field of view. The imaging optics cover a circular field of view of 1.5 deg with an all-reflective, highly corrected anastigmatic design using nickel-plated aluminum mirrors. The focal plane is actively cooled to 40 K for optimum performance. The AMS and its image analysis electronics and subpixel centroid algorithm provide absolute target position to an angular accuracy of $3.5 \mu\text{rad}$. The AMS is used to provide calibrated target tracking to position uncertainty within the field of view (FOV). The data noted in the next section indi-

cate considerable improvement over the original calibration.

In addition to goniometric calibration, the AMS is an invaluable tool for diagnosing problems such as stray light, narcissus, and target output. Using the increased sensitivity at long integration times, the InSb focal plane has helped detect stray light problems by identifying faint signals from target glints and reflections from warm seekers. Some of the results on decreasing stray light are shown in the section on Facility Test Results.

OPTICAL SIMULATION

The Chamber Optical System, shown in Fig. 1, provides collimation of the calibration or scene output, target selection, and single-axis azimuth scanning for high-speed target movement and alignment. The 7V collimator is a two-mirror, off-axis Cassegrain constructed from nickel-plated aluminum for cryogenic operation and low scatter performance. The focal length is 1,645 cm, providing a collimated beam of greater than 50-cm diameter with a circular field of view (FOV) of 1.4 deg. The mirrors are coated with enhanced silver with a protective overcoat, providing reflectance of greater than 0.97 from 0.4 to at least $30 \mu\text{m}$. Both the primary and secondary mirrors mount independently to the 7V optical bench on actively cooled, massive aluminum structures. Optical quality of the collimator was measured interferometrically at 20 K, indicating diffraction-limited performance over the full 50-cm beam at $5 \mu\text{m}$. For seeker testing, smaller areas of the collimator are even better, being diffraction-limited to less than $2 \mu\text{m}$.

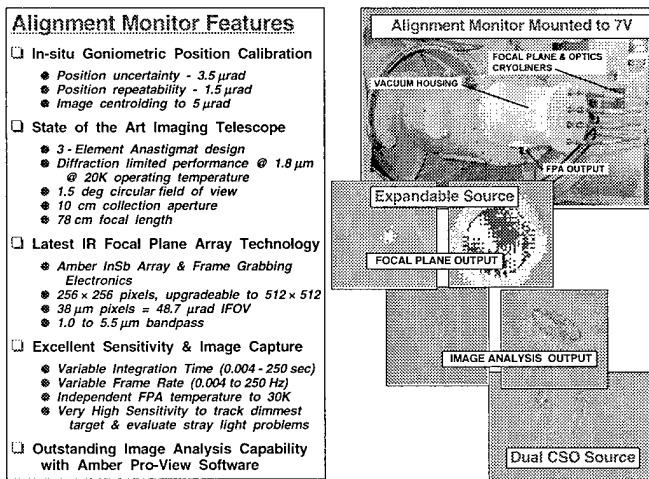


Fig. 10. Alignment Monitor Goniometric Calibration System.

UNCLASSIFIED

The scan mirror, mounted between the sources and the collimator secondary, provides high-speed azimuth sweep of the targets across the seeker's FOV. The light-weighted aluminum mirror rotates about a vertical axis on two stainless flexure pivots. The mirror is driven by a brushless DC servo motor with closed-loop position control from a brushless Inductosyn® encoder. In collimated space, this system can sweep a target completely across the field of view at rates from 0 to 6 deg/sec with position knowledge and resolution of ± 0.5 μrad.

The 7V Optical System was modeled using CODE V® and validated using interferograms measured during the acceptance test of the collimator. Unfortunately, due to access and space limitations within the 7V vacuum chamber, a full system optical evaluation cannot be made with an interferometer. To obtain some information on the optical performance of the complete optical train at cryogenic conditions, an attempt was made to measure the point spread function (PSF) using the AMS. The preliminary results are given below.

FACILITY TEST RESULTS

RADIOMETRIC CALIBRATION RESULTS OF 7V IR SOURCES

The 7V Radiometric Calibration System and all the target sources have undergone extensive calibration using NIST-traceable standards to establish excellent radiometric accuracy and repeatability during eight separate tests over the last three years. The methodology used at AEDC is an end-to-end approach using the calibration monitor as a broadband and spectral radiometer to image any of the 7V IR sources onto its Si:Ga detector. The irradiance from the collimated source, E , is a function of the source radiance, L , the source output aperture area, A_s , an attenuator throughput, T_r , and the collimator focal length, f , as formulated in the following equation

$$E = \frac{A_s T_r}{f^2} L \quad (1)$$

The blackbody radiance, L , is a function of the source temperature, T , and radiation wavelength, λ , as formulated in Planck's radiation equation and spectrally integrated in Eq. (2). The in-band radiance is calculated as an integral between specified wavelength limits.

$$L = \frac{1}{\pi} \int_{\lambda_1}^{\lambda_2} \frac{c_1}{\lambda^5 \left(e^{c_2/(\lambda T)} - 1 \right)} d\lambda \quad (2)$$

where: $c_1 = 37418.32 \text{ W cm}^{-2} \mu\text{m}^4$
 $c_2 = 14387.86 \mu\text{m K}$

For real radiation sources, collimation systems, and attenuators, the effective irradiance, E_{eff} , of the collimated source is a function of the effective source radiance, L_{eff} , the source output aperture area, A_s , the system's peak throughput, $T_{p,\lambda}$, and the collimator focal length, f , as formulated in Eq. (3)

$$E_{eff} = \frac{A_s T_{p,\lambda}}{f^2} L_{eff} \quad (3)$$

All of the constants on the right side of Eq. (3), except the variable L_{eff} , can be combined into a single source calibration constant, K . Because most sources have multiple source apertures, a source constant is defined for each of the apertures as $K(A_s)$, by Eq. (4) as the ratio of the effective irradiance to the effective radiance.

$$K(A_s) = \frac{E_{eff}}{L_{eff}} \quad (4)$$

The source's effective radiance, L_{eff} , includes the collimator system's relative spectral throughput, $T_R(\lambda)$, and is calculated using Eq. (5)

$$L_{eff} = \frac{1}{\pi} \int_{\lambda_1}^{\lambda_2} \frac{T_R(\lambda) c_1}{\lambda^5 \left(e^{c_2/(\lambda T)} - 1 \right)} d\lambda \quad (5)$$

The system peak throughput, $T_{p,\lambda}$, contained in Eq. (3) includes the peak normalized values of the source emissivity, the collimator mirror reflectance, and any attenuator throughputs. The relative spectral throughput is contained in $T_R(\lambda)$ and includes the relative spectral values (normalized by the peak values) of the source emissivity, the collimator mirror reflectance, and attenuator throughputs. For sources that are attenuated with integrating spheres, all of the relative spectral and peak throughputs can be combined into one set of parameters. If neutral density (ND) filter attenuation is used, the relative spectral and peak throughputs of each filter are generally separated from the combined system values.

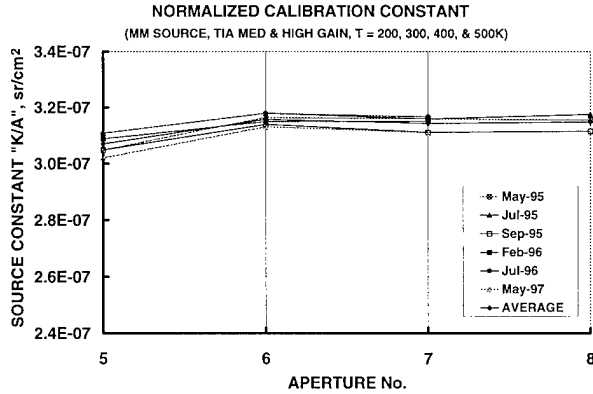


Fig. 11. RCS multimode source calibration results.

Calibration results acquired to date on the RCS Multi-Mode Source (MMS) are shown in Fig. 11. These data show the calibration constant, K , normalized by the source pinhole area A_S , plotted for the four pinholes in the MMS. To illustrate the excellent repeatability and accuracy of radiometric performance of the 7V sources, each plotted point is an average of all data (over 150 points covering two detector gains and the complete source temperature range from 200 to 500 K) taken for a given aperture during six separate pumpdowns covering two years. The total spread in these data is less than 2 percent with a standard deviation of less than 1 percent. The dip for aperture 5 (0.64 mm) data represents a systematic error in the assumed area of the pinhole, not an error in the calibration constant. Complete results³ indicate that the overall radiometric uncertainty for both the RCS Multimode and Unisphere sources is less than 3 percent with worse case repeatability of 2.8 percent for 17 separate measurements.

RADIOMETRIC CALIBRATION OF THE CRISP SCENE GENERATOR

A two-color approach was used to calibrate the CRISP array. All pixels in the 512×512 CRISP array were calibrated using the AMS and an extensive calibration sequence. The results from one frame of the calibration sequence are shown in Fig. 12. A select group of pixels was calibrated using the CMS to provide an independent assessment of the operating temperature of the CRISP pixels at selected voltage settings. A plot of pixel temperature versus gate voltage setting for 11 pixels is shown in Fig. 13. Using the AMS data, the response characteristics for all pixels in the array were determined over an appropriate gate voltage range. The results were compiled into an overall

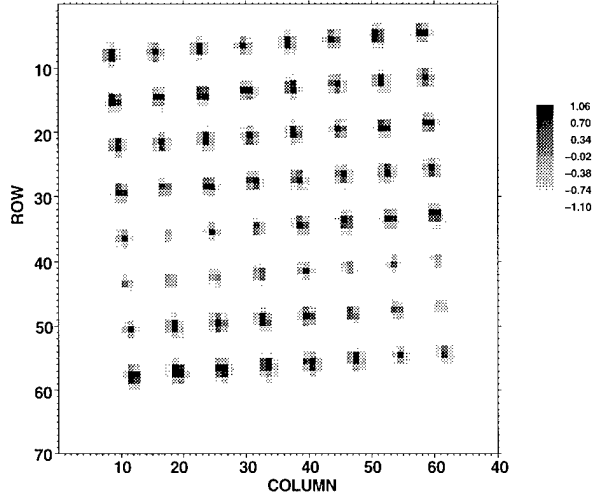


Fig. 12. CRISP radiometric calibration data frame.

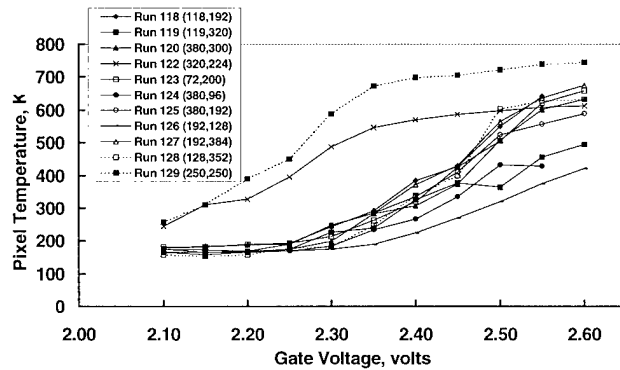


Fig. 13. CRISP pixel temperature vs. gate voltage.

response map that indicated that 98.6 percent of the CRISP pixels were operable. The calibration results were used to develop scene projection files that presented targets at the desired radiance for the seeker mission simulation.

IMPROVED GONIOMETRIC TRACK CALIBRATION

Validating the target track accuracy requirement of $5 \mu\text{rad}$ has been challenging. The initial attempt to calibrate the X-Y target scan table resulted in $7 \mu\text{rad}$ (1σ) over the 0.75-deg core field covered by the AMS camera and $9 \mu\text{rad}$ "boot strapped" over the entire 1.2-deg-square field covered by the scanner. It was suspected that the problem was in the calibration scheme and not the hardware. After careful review, the most likely causes were traced to (1) jitter/non-repeatability in the Monitor Selector Mirror drive, and (2) a bad nonuniformity correction (NUC) of the AMS focal plane. After correcting these two problems, the calibration was rerun.⁴ Figure 14 shows the output of

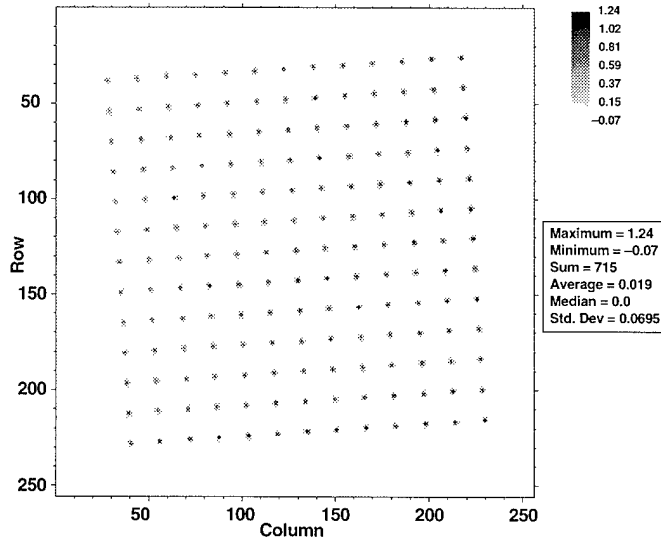


Fig. 14. X-Y scanner goniometric calibration.

a 13×13 (approximately 6-in.) point scan over the core field. The position of each of the 169 data points is defined by the output of the two Inductosyn encoders on the X-Y scanner. The measured position is calibrated by the AMS camera, which calculates a radiometric centroid of each $15\text{-}\mu\text{m}$ target (based on pixel outputs from a 5×5 subarray). The difference in these two values is the position error which includes all effects (mechanical, optical, and measurement errors). The total error (1σ) in x, y position is $4 \mu\text{m}$.

DECREASED NARCISSUS FROM WARM SEEKERS

Testing of seekers with warm optics causes special problems in any low-background chamber. Radiation from the uncooled surfaces of the seeker adds significantly to the chamber background and presents the potential of inducing target clutter. Considerable work was done to evaluate the problem for specific seeker tests and reduce it to acceptable levels. Ray trace analysis and inspection with high-intensity lights and a camera, along with data taken by the AMS and the RCS during several pumpdowns and seeker data from two tests, were used to diagnose and minimize the problem. Figure 15 contains one example of a before and after image of the target clutter problem caused by illumination from the warm optics of a test seeker. The upper pair of figures shows the RCS Multimode calibration source and its corresponding image on the seeker focal plane. In this case, the clutter is comparable to the brightest target. In the lower set, new shields on the front of the

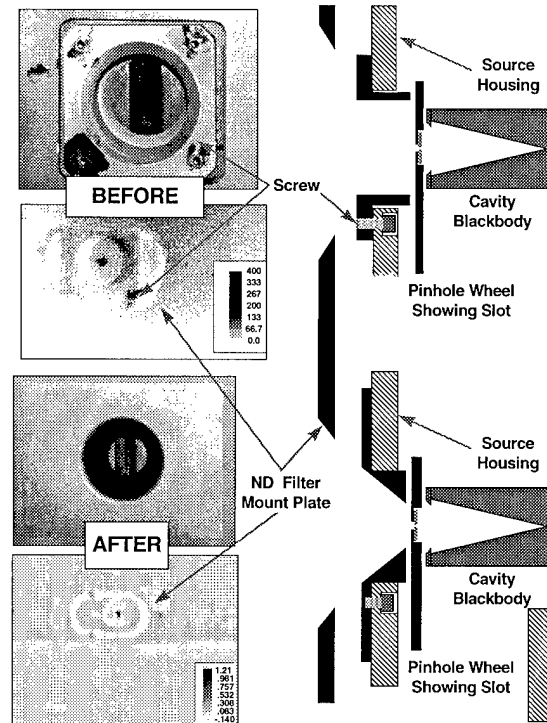


Fig. 15. Example of improved target clutter.

source and baffling on the seeker reduced the clutter to negligible levels that are less than one of the dimmest target. The basic approach involved (1) reducing the view factor of the warm seeker into the chamber by minimizing the size of the cold baffle shielding the seeker and, (2) reducing sharp edges, and eliminating bolt heads and other scattering surfaces in the source area.

SPECTRAL CHARACTERIZATION OF TARGETS

The CVF wheel in the RCS calibration monitor was used to spectrally calibrate all sources in the 7V Chamber. However, the spectral range associated with the three-segment *in-situ* CVF is limited to a maximum wavelength of $14.5 \mu\text{m}$. During the latest checkout, an independent CVF spectrometer with segments out to $22.5 \mu\text{m}$ was used to acquire spectral data for the multimode calibration source and the CRISP over a 50 percent larger range. The results for the multimode source are shown in Fig. 16. The results confirm earlier measurements which indicate there are no unexpected anomalies in the spectral output at longer wavelengths.

OPTICAL SYSTEM VALIDATION

An attempt was made during the last 7V cold test to validate the complete 7V optical system with

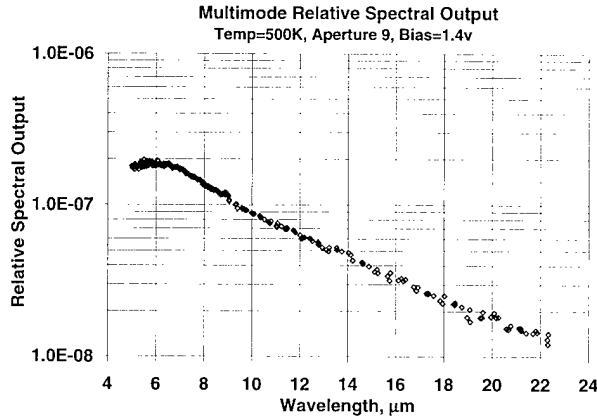


Fig. 16. Extended spectral measurements for typical source.

an end-to-end measurement of its point spread function (PSF). Although preliminary and insufficient data were obtained on the first attempt, the data provide an approximation of the rms wavefront error of the facility including the effects of all optical elements. The approach used to measure the overall PSF, as shown in Fig. 17, is basically a knife-edge scan of the energy from a "monochromatic point source." The source used is one of the CSO blackbodies with a 15-mrad pinhole with a narrow-band filter near the maximum response of the InSb FPA. Using the effective bandwidth of 0.37 mm (6.8 percent at 5.38 mm) and the AMS entrance aperture of 11 cm, the theoretical PSF dimension is about 120 μ rad. Because the small geometric size and narrow bandwidth of the source minimize the contributions to the PSF growth, the knife-edge energy distribution provides a reasonable measurement of the 7V PSF and optical quality.

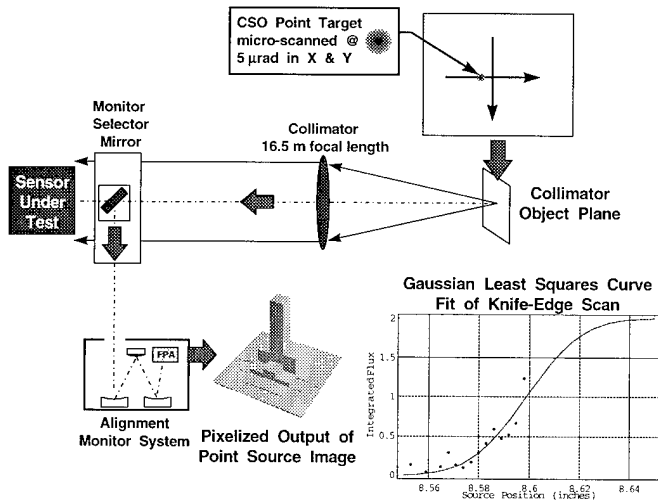


Fig. 17. PSF measurement concept.

The integrated output of the scanned target image, as measured by the AMS, is plotted in Fig. 17 against the source position. In order to obtain the PSF from this energy distribution, a closed-form Gaussian approximation is used for the Bessel-distributed PSF to obtain a least-squares curve fit of the knife-edge data. Converting this energy distribution into a PSF size and ratioing against the theoretical value indicates a 6.4 percent increase in the 7V optics 84-percent blur diameter. The corresponding reduction in the peak PSF intensity or Strehl ratio is 0.88, which corresponds to approximately a 1/14 wave rms wavefront error or diffraction-limited performance at wavelengths comparable to or larger than the 5.38- μ m mean wavelength used.

SUMMARY

The 7V Facility provides an advanced test capability for seeker sensors with full calibration capability traceable to NIST, complete seeker characterization over a full mission envelope, and high-fidelity simulation of all critical seeker mission phases in real time. The 7V optical system, calibration accuracy, and scene simulation are state of the art. With modernized control rooms, environmental systems and data systems, the 7V Facility provides a ground test capability unmatched anywhere for complete evaluation of the next generation of infrared interceptors.

REFERENCES

1. Simpson, W. R., "Seeker Testing in AEDC'S 7V Sensor Test Chamber," AIAA/BMDO 4th Technology Readiness Conference, Natick, MA, July 1995.
2. Mead, K. D., Nicholson, R. A. and Simpson, W. R., "Recent Evaluation and Test Activities in the AEDC 7V Chamber," 7th SDL/USU Symposium on Infrared Radiometric Sensor Calibration, May 1997.
3. Selman, J. D., Goethert, W. H., Dawbarn, R., "Analysis of an Earth Limb Simulator for the AEDC Aerospace Chambers 7V and 10V," 42nd International Instrumentation Symposium, San Diego, CA. May 1996.
4. Nicholson, R. A. and Mead, K. D., Kiech, E. L., "Calibration of a Complex Scene Generator in the AEDC 7V Chamber," 7th SDL/USU Symposium on Infrared Radiometric Sensor Calibration, May 1997.